EUROPEAN ORGANIZATION FOR NUCLEAR RESEARCH
European Laboratory for Particle Physics

Large Hadron Collider Project

LHC Project Report 905

Identification of Assembly Faults through the Detection of Magnetic Field Anomalies in the Production of the LHC Dipoles

C. Vollinger, E.Todesco

Abstract

Magnetic measurements at room temperature have been used to monitor the production of the superconducting coils of the Large Hadron Collider main dipoles. They have made it possible to identify several assembly errors, e.g. cases of bad gluing of the coil layers, bad conductor positioning, missing pole shims and other problems related to faulty procedures. This paper reviews the experience accumulated so far considering almost 1000 dipoles. After a short outline of the method used to pin out field anomalies and deduce realistic deformation of the coil, an exhaustive list of the cases met during the production is given. A discussion follows on the findings after decollaring as compared to the predictions, including the still open cases.

CERN, Accelerator Technology Department, Geneva, Switzerland

Presented at the 19th International Conference on Magnet Technology (MT19)
18-23 September 2005, Genova, Italy

CERN
CH - 1211 Geneva 23
Switzerland

Geneva, 19 May 2006

Identification of Assembly Faults through the Detection of Magnetic Field Anomalies in the Production of the LHC Dipoles

C. Vollinger, E.Todesco

***Abstract*—Magnetic measurements at room temperature have been used to monitor the production of the superconducting coils of the Large Hadron Collider main dipoles. They have made it possible to identify several assembly errors, e.g. cases of bad gluing of the coil layers, bad conductor positioning, missing pole shims and other problems related to faulty procedures. This paper reviews the experience accumulated so far considering almost 1000 dipoles. After a short outline of the method used to pin out field anomalies and deduce realistic deformation of the coil, an exhaustive list of the cases met during the production is given. A discussion follows on the findings after decollaring as compared to the predictions, including the still open cases.**

***Index Terms*—LHC, Superconductivity, Field Quality, Accelerator Magnets**

I. Introduction

In superconducting magnets for particle accelerators [1,2], the shape of the magnetic field is determined by the position of the conductors, and is a powerful indicator of the actual geometry of the coils inside the magnet. Therefore, magnetic measurements at room temperature can be used like X-rays to determine if the magnet has been assembled in a correct way. This has been done during the production of the magnets of the Relativistic Heavy Ion Collider [3], where field measurements have been used to perform a sophisticated quality control and is now applied to the main Large Hadron Collider (LHC) dipoles. In this paper we present the method that has been used to single out field anomalies for the production of the LHC main dipoles and to trace them to assembly errors. This method has been successfully applied to screen almost 1000 magnets (approximately ¾ of the LHC dipole production), allowing to detect 15 cases of faulty components or wrong assembly procedures.

II. The main LHC dipole coil layout

The assembly of the main LHC dipoles is carried out at three manufacturers. The magnet has two apertures held in a common mechanical structure (the stainless steel collars). Each superconducting coil is assembled around a 56 mm diameter aperture according to the cosine-θ layout (see Fig. 1). The coil geometry has a four fold symmetry, where current is flowing in opposite directions in the left and right part of the aperture. Each coil is made up of two layers with a different type of cable. In each quarter of the coil, conductors are assembled in four and two blocks in the inner and outer layer, respectively. Spacers are present on the coil poles, and a shim of insulating tape is put in the mid-plane. The typical order of magnitude of the precision in the cable positioning in the cross-section is 100 μm.

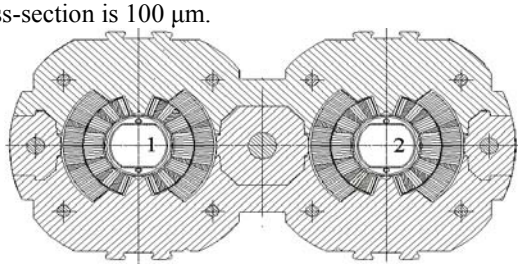

Fig. 1. Sketch of the collared coil (coils clamped in austenitic steel collars) of the main LHC dipole with the two apertures in one common structure.

III. Warm magnetic measurements

The magnetic field in a dipole is expressed as a power series

$$B_y(x,y)+iB_x(x,y)=10^{-4}B_1\sum_{n=1}^{\infty}(b_n+ia_n)\left(\frac{x+iy}{R}\right)^{n-1}$$

where (x,y) are the transverse coordinates, R is the reference radius (17 mm in our case), and B_1 denotes the main dipolar component. The multipolar terms (b_n,a_n) have a main component b_1 which is 10^4 by definition; the terms b_3, b_5, b_7 … are generated by a coil layout that satisfies left-right and the up-down symmetry ("allowed" components), whereas the other terms are due to a break of these symmetries ("not allowed" components). The main component and the field harmonics are measured at room temperature with a rotating coil of 750 mm length, along 20 consecutive positions to cover the 14.3 m long dipole. Position 1 and 20 cover the ends of the coils, and 2 to 19 the so-called straight part. Measurements are carried out at the manufacturer at two stages of the assembly procedure, namely after the collaring (superconducting coils clamped in the collars), and after the welding of the shrinking cylinder (the so-called cold mass, i.e. the collared coil inside the iron yoke and welded in a stainless steel vessel). If field anomalies with variable patterns along the magnet axis are detected, a special measurement is done with a shorter mole (125 mm) in order to have a higher spatial resolution.

Manuscript received September 21, 2005.

All authors are with CERN, Geneva, Switzerland (corresponding author C. Vollinger, email: Christine.Vollinger@cern.ch, Tel: +41 22 7671062), Fax: +41 22 7676300.

IV. The Method for Defect Detection

The method for defect detection follows two logical steps: the identification of the magnetic field anomalies in a certain position along the magnet axis, and the evaluation of the coil movement that can produce that field anomaly.

To single out field anomalies, one has to set control limits over the field harmonics. We established such control limits for the magnetic field at an early stage of the production (30 collared coils). These limits have been updated with the data of 300 collared coils in a mature phase of the production. After rejecting faulty measurements or magnets with known anomalies, data have been separated according to the cold mass assembler. Moreover, for each set of measurements, data are split into average values along the straight part, variation along the straight part, and coil heads. For each subset, the average μ and the standard deviation σ of each multipole are evaluated. Control limits are then set for each subset as a range centered on the average with a width of 4 standard deviations. A multipole out of this range is considered as anomalous, triggering a "yellow alarm". We choose 4σ since in this way, in the hypothesis of a Gaussian production without field anomalies, one has only one case out of the control limits over all the production of 2400 apertures, i.e. one false alarm, for each multipole. We also defined a second range, with a double width of 8σ, to point out very strong field anomalies ("red alarms").

For each multipole, the field anomaly is expressed as the difference between the measured value and the average, divided by the standard deviation

$$\beta_n \equiv \frac{b_n^{\text{meas}} - \mu_{b_n}}{\sigma_{b_n}} \qquad \alpha_n \equiv \frac{a_n^{\text{meas}} - \mu_{a_n}}{\sigma_{a_n}} \tag{2}$$

where n is the multipole order, running from 1 to 15 in our case. The normalization to the standard deviation is a natural way to define a coherent weight for each multipole, thus allowing to comparing anomalies of different multipoles. We point out that the determination of weights is always a critical point for two typical inverse problems, such as tracing field anomalies to coil displacements [4], and optimizing the coil lay-out with respect to multipoles [5]. In the literature, weights are often chosen on the basis of experience and/or by iteration; the proposed Eq. (2) sets a simple and objective rule to set weights for the inverse problem related to coil displacements. We also point out that the used spread is not related to the beam dynamics targets, but only to the outcome of the production. The anomaly γ is then computed as the maximum of the anomalies (β_n, α_n) over all multipoles. We believe that the norm of the max is more suitable than the Euclidean norm (sum of the squares) which is commonly used: in this way the condition to have a field anomaly simply reads as $\gamma > 4$. Its disadvantage is that, being not differentiable, not all the minimization algorithms can be applied.

The second delicate aspect of the problem is the selection of the coil movements that can be the source of the measured field anomaly. Since there are numerous possibilities for coil displacements, it is impossible to have an exhaustive exploration because too many degrees of freedom are involved. On the other hand, physical constraints make most of the displacements "unlikely". Thus, we selected the following list of K coil displacements compatible with the coil assembly: radial displacement of each of the conductor blocks, combinations of blocks or complete layers, and a different thickness of the shim on the coil pole or on the mid-plane (inner and outer layer separately). Each case k=1, K gives rise to a multipole shift $\Delta c_{n,k}(\lambda)$, which is linear in the amplitude λ of the displacement for the range of interest for this problem (0.05 to 1 mm). Even though our library of coil displacements obtained this way is very limited, we will show that most of the cases could be understood in terms of these movements.

For each multipole and coil movement, one can define the residual anomaly

$$\beta_n^r(k,\lambda) \equiv \left| \frac{b_n^{\text{meas}} - \mu_{b_n} - \Delta b_{n,k}(\lambda)}{\sigma_{b_n}} \right| \tag{3}$$

that is the fraction of the multipole anomaly which is not explained by the coil displacement, expressed in units of σ; a similar formula holds for the residual anomaly α^r_n of the skew components. The coil movement and amplitude that minimizes

$$\gamma^r \equiv Min_{k,\lambda}\left(Max_n\left(\beta_n^r(k,\lambda), \alpha_n^r(k,\lambda)\right)\right) \tag{3}$$

i.e., the maximum of the residual anomaly over the multipoles is our solution. If the residual anomaly γ^r is less than 4, it means that the coil displacement completely accounts for the field anomaly. A very important point is that we do not try to get γ^r=0, which could create unphysical solutions since it aims at a perfect coil geometry. Instead, we look for solutions giving γ^r<4, i.e. we aim for bringing back the field anomaly within the statistics. In the following we will show cases with field anomalies in the range of 5 to 10, where coil movements could be predicted to obtain a residual anomaly below 4. Usually, magnets were de-collared only for coil movements larger than 0.3 mm.

V. Detected Assembly Errors in the LHC Main Dipoles

A. Wrong assembly procedures

The missing shim: Fig. 2 shows the measurement of b_2 with a yellow and red alarm corresponding to field anomalies of 6.6 and 9.2 (see circle on the plot). The inverse calculation indicated that an increase of the coil size azimuthally of about 0.6 to 1 mm on the outer layer gives a residual anomaly within 4. This was suggesting a missing shim in the outer layer pole, whose thickness is 0.8 mm. This prediction was confirmed by the de-collaring (Fig. 3). We have observed one case of a missing pole shim so far.

The sliding shim: Fig. 4 shows the measurement of multipole b_6 indicating a yellow alarm from the standard measurement (triangle markers) and red alarms from the short mole measurement (see arrow indicator). On this collared coil, alarms on various multipoles were observed in the last measurement position in the straight part before the non-connection side coil end (see the anomaly of the lower order multipoles in tab. I).

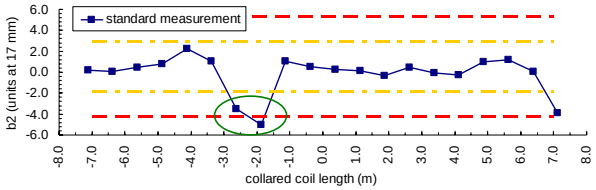

Fig. 2. Measurement of multipole b2 along the magnet axis with alarm limits at 4σ and 8σ (dashed lines) for a collared coil with missing pole shim.

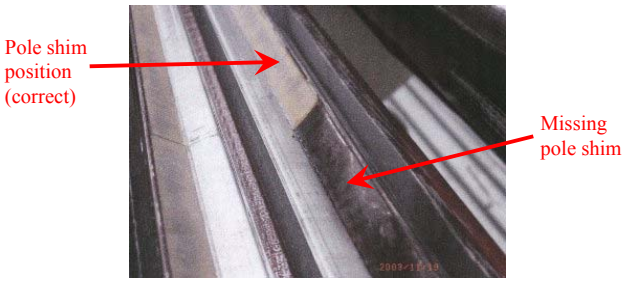

Fig. 3. Missing pole shim observed after de-collaring.

TABLE I
MEASURED MULTIPOLES ANOMALY IN THE DEFECT POSITION

b_n	2	4	6	8	a_n	2	4	5	7
β	7.5	4.9	5.5	5.9	α	5.5	6.8	5.5	5.2

The inverse calculation of the values in table I shows that a movement of block 5 of about 0.3 mm together with a movement of block 6 of about 0.6 to 1 mm, both radially inwards, would give a residual anomaly within 4. Please note that a movement of one block only does not explain the anomaly. After de-collaring, we observed that an outer pole shim of 0.8 mm thickness had slid downward, pushing blocks 5 and 6 towards the centre of the aperture as shown in Fig. 4. On the right side of Fig. 5, it is illustrated in three steps how the pole shim is sliding onto the conductor blocks 5 and 6. We have observed two cases of a sliding pole shim so far.

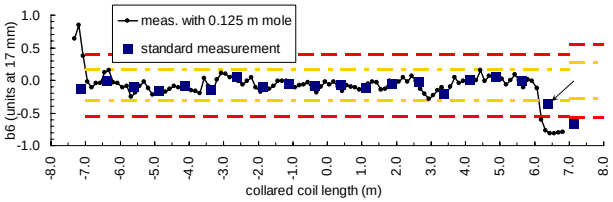

Fig. 4. Measurement of multipole b6 along the magnet axis with alarm limits at 4σ and 8σ (dashed lines) for a collared coil with a misplaced pole shim.

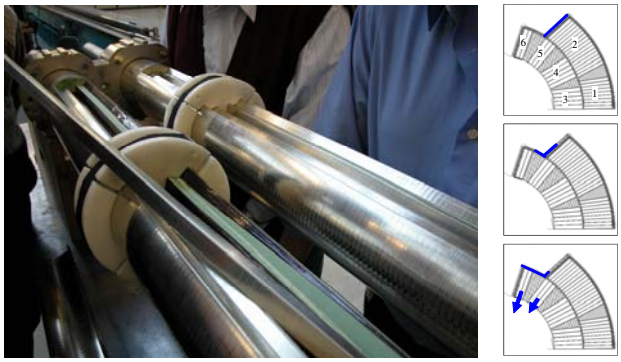

Fig. 5. Left: Movement of blocks 5 and 6 of the inner layer of the coil observed after de-collaring due to a misplaced pole shim of 0.8 mm thickness. Right: Illustration of the predicted defect and block numbering.

The double coil protection sheet: This was the fourth magnet of the production, and the control limits had not yet been set. A very strong anomaly in the main field (40 units) was observed along 0.75 m in the central part of the magnet, associated to a peak in b_2 (see Fig. 6). The inverse calculation methods were not yet set. Due to the amplitude of the anomaly, the magnet has been decollared, finding a double coil protection sheet of 0.5 mm thickness on a length of 1 m in this measurement position (see Fig. 7). Simulations of the effect of this error on field quality done a posteriori are in agreement with the measured anomaly. We have observed one case of a double coil protection sheet so far.

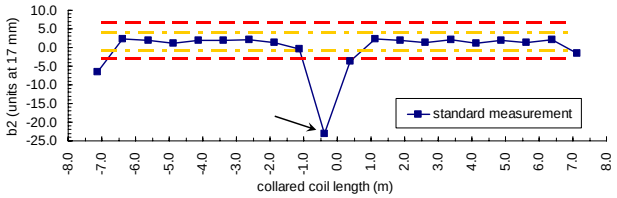

Fig. 6. Measurement of multipole b2 along the magnet axis with alarm limits at 4σ and 8σ (dashed lines) in the straight part.

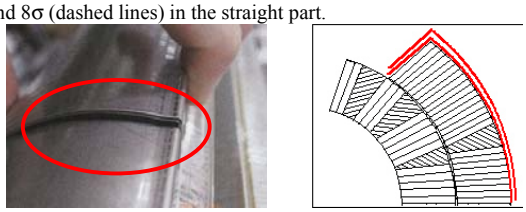

Fig. 7. Assembly of a double coil protection sheet observed after de-collaring (left); illustration of the defect (right).

B. *Faulty manufacturing process or component*

Bad coil curing: Conductor displacements in block 6 due to a bad curing of the coil could be identified by individual multipole alarms in isolated positions along the axis. In several cases, the standard measurement was followed by a special measurement using the 0.125 m long coil to have a better resolution along the magnet axis. The longitudinal size of these defects proved to be rather small (0.01 to 0.02 m).

An inward radial displacement of block 6 in one quadrant mainly affects a_6 and b_8. Fig. 8 shows the measurement of multipole b_8 taken on a collared coil with a standard and a detailed measurement (triangle markers and continuous line). The field anomaly of the short mole measurement is very strong, i.e., up to 12- 13. For the two positions indicated with arrows, an inverse calculation of the pattern of all multipoles in this position indicated an inward radial movement of block 6 of 0.5 to 0.8 mm. Fig. 9 shows one of these positions after decollaring: block 6 is found not to be glued to the inner layer, thus leading a inward displacement in the assembly. We have observed 7 cases of bad curing so far. Corrective actions have been taken in the curing cycle to avoid this problem.

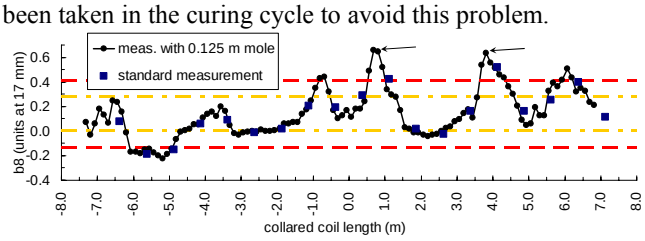

Fig. 8. Measurement of multipole b8 along the magnet axis with alarm limits at 4σ and 8σ (dashed lines) for a collared coil with curing problem.

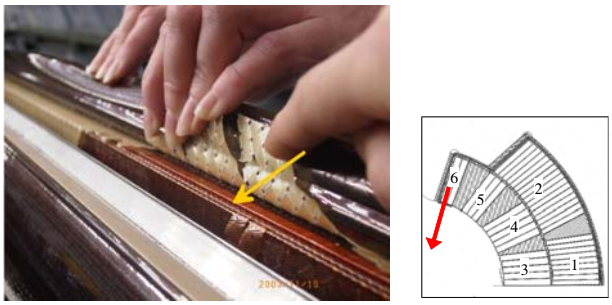

Fig. 9. Left: Movement of block 6 of the inner layer of the coil observed after de-collaring. Right: Illustration of the predicted defect and block numbering.

Magnetic anomalies in the cold bore tube: One collared coil showed yellow and red alarms on various multipoles, especially on the higher orders (see Table II), of which one of the strongest signals, multipole b_9, is shown in Fig. 10. From the calculation, no solution was found, but the very strong impact on high orders suggested that the source of the error was very close to the centre of the aperture, even closer than the inner layer. For this reason, the magnet was reassembled with the cold bore rotated (connection side at the place of non connection side). A second measurement showed that the defect had changed longitudinal position. The tube was then removed, and a permeability measurement showed an out of tolerance over the expected section. We have observed two cases with a faulty cold bore tube. Even though this field perturbation is not endangering the beam, in both cases the cold bore tube has been replaced.

TABLE II
MEASURED MULTIPOLES IN DEFECT POSITION INDICATING THE DEFECT CBT

b_n	4	6	9	11	a_n	6	7	8	11
β	8.2	11.1	16	10.1	α	7.1	10.7	15.3	12.2

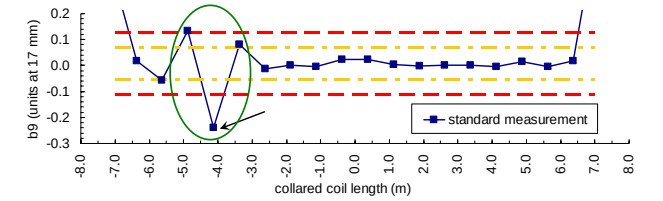

Fig. 10: Measurement of multipole b9 along the magnet axis with alarm limits (dashed lines) for a collared coil with a defect in the material features of the circular cold bore tube (CBT).

C. *Open cases – no defects found*

Curing problems: Fig. 11 shows magnetic measurements along the axis of b_8 (bottom) in a collared coil. The field anomaly was compatible with a radial movement of block 6 of 0.4 mm. This case looked very similar to the curing problem described in the previous section. However, after de-collaring, a movement of block 6 of only 0.15 mm could be observed.

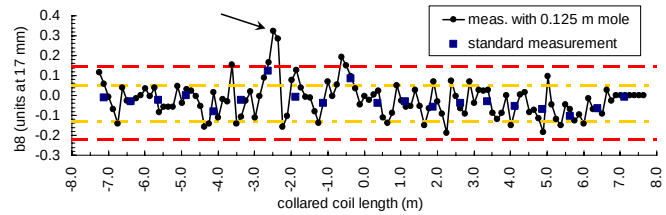

Fig. 11. Measurement of multipole b8 along the magnet axis with alarm limits for a collared coil with an expected block 6 movement.

In a second case, from the measurement of multipole a_6 shown in Fig. 12 (see arrow), a conductor movement of block 6 radially inwards of about 0.3 mm was predicted from inverse calculation and a curing problem was also suspected. After de-collaring, we observed that the curing was fully intact. However, block 6 was ill-positioned, *i.e.*, it was glued to the adjacent copper wedge with a radial movement towards the center of the aperture of about 0.1 mm. The amplitude of the visible movement did not match the prediction. In a third similar case, no visible block 6 displacements were observed.

The most probable explanation for these cases is that block 6 was misplaced during the collaring but correctly glued, and that after de-collaring it springed back to the original position.

Anomaly in a_2: Fig. 12 shows the field anomaly that was measured for a_2 in one collared coil. The absence of anomaly on the high orders suggested that the defect is located in the outer layer. Even though no solutions were found, the magnet has been de-collared since the anomaly was very strong (more than 11 σ). The de-collaring has shown no visible defect. This case is hard to judge since no solution was available, and therefore no estimate of the coil movement was possible.

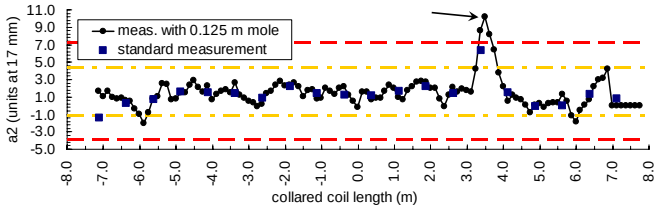

Fig. 12. Measurement of multipole a2 along the magnet axis with alarm limits (dashed lines) for a collared coil with an expected pole shim problem.

VI. CONCLUSIONS

We presented the method that has been used to detect field anomalies and to relate them to assembly errors. 17 cases of wrong assembly or faulty components have been detected at the level of the collared coil: in 13 cases the expected defect was found, allowing to rescuing the magnet in a very early stage of the production and to improve the assembly procedures.

We had four cases of wrong assembly procedures such as missing pieces, double pieces, or parts not assembled correctly. In seven cases, a bad curing of the coil has been detected, and two faulty components (cold bore tube) have been found. In four cases, the expected movement of the conductors was found to be much smaller or absent. In most of these cases it is probable that the predicted displacement disappeared after de-collaring.

REFERENCES

[1] M. N. Wilson, "Superconducting Magnets", Clarendon Press, 1983.
[2] K. M. Mess, P. Schmüser, S. Wolff, "Superconducting Accelerator Magnets", World Scientific Publishing, 1996.
[3] R.C. Gupta, et al., "Field Quality Analysis as a Tool to Monitor Magnet Production", Proc. 15th International Conference on Magnet Technology (MT15), Science Press, Beijing, China (1997) 110.
[4] S. Russenschuck, ed., *CERN Yellow Report* **99-01** (1999) 184.
[5] S. Russenschuck, ed., *CERN Yellow Report* **99-01** (1999) 22, 86.